ORIGINAL ARTICLE

Accuracy Improvement of 3D Models Generated

by Structure from Motion (SfM)

Using Joint Histogram of Oriented Gradients (Joint-HOG)

Reika Yamaguchi[1*], Nobuyoshi Yabuki[1], Tomohiro Fukuda[1]

[1] Division of Sustainable Energy and Environmental Engineering, Osaka University
2-1 Yamadaoka, Suita, Osaka, 565-0871, JAPAN

[*] E-mail: yamaguchi@it.see.eng.osaka-u.ac.jp

Abstract: This study investigates the potential of 3D modeling of construction sites with high precision. Structure from Motion (SfM) combined with Unmanned Aerial Vehicle (UAV) provides a novel platform for photogrammetry. In construction industry, research and development have been promoted for practical use in automatically quantity calculation and obtaining its as-is forms. Nothing in the shooting area of any construction sites must not move during the UAV aerial shooting. Because moving construction machinery cause serious errors in 3D modeling. Hence, it is necessary to stop all works while UAV aerial shooting. As it can take a few hours for UAV aerial shooting, it is difficult to shoot frequently at construction sites. Therefore, by eliminating construction machinery which are error factors of 3D modeling automatically from all photographs taken in advance in UAV aerial photography, it is possible to realize highly accurate 3D modeling even under work conditions. Construction machinery can be detected by Histgrams of Oriented Gradients (HOG) features. HOG features calculate the intensity of the gradient for each gradient direction in the region, expressed as a histogram. It is possible to extract the boundary line of change in luminance in the image. However, using single HOG features ends up to have low detection accuracy. In this paper, the authors deployed Joint-HOG features combined with multiple HOG features by Real AdaBoosting which was constructed in two stages in order to detect construction machinery. Then, a 3D model of the construction site is created by SfM, after generating mask image of objects that showed be eliminated, detecting construction machinery.

1. Introduction

In recent years, Structure from Motion (SfM) combined with Unmanned Aerial Vehicle (UAV) provides a novel platform for photogrammetry. 3D modeling combining SfM and UAV is used for grasping the damage situation of buildings in the afflicted earthquake area[1] and for measuring tree height of forest trees[2]. In construction industry,

research and development have been promoted for practical use in automatically quantity calculation and obtaining its as-is forms. The 3D modeling of the construction sites with SfM is expected to improve the productivity of the construction sites.

Despite all the benefits, there are still problems to realize practical use. The main reasons are as follows.

On any construction sites, a lot of construction machinery are constantly working and moving around. Nothing in the shooting area of any construction sites must not move during the UAV aerial shooting. Because moving construction machinery cause serious errors in 3D modeling. Hence, it is necessary to stop all works while UAV aerial shooting. And as it can take a few hours for UAV aerial shooting, it is difficult to shoot frequently at construction sites. Therefore, by eliminating construction machinery which is an error factor of 3D modeling automatically from all images taken in advance in UAV aerial photography, it should be possible to realize highly accurate 3D modeling even under work conditions.

In this study, Histograms of Oriented Gradients (HOG) features are obtained from the image taken during UAV aerial shooting, and Joint-HOG features[3] calculated based on the combination of the HOG features for each cell are employed to detect the construction machinery, and a mask image was created for each image, thereby removing construction machinery from the 3D modeling target. And at the construction site, a demonstration experiment of the proposed method was conducted.

2. Related work

In recent years, interest in the diversity of 3D modeling technology combining SfM and UAV is increasing. This is mainly due to the low cost, fast speed, high maneuverability, and high safety of UAV

systems for collecting images. In addition, studies are also being conducted to automatically detect construction machinery using various features from images taken at construction sites.

2.1 Construction sites 3D modeling

To date, much research on UAV system has been conducted. They are used for grasping damage situation at the time of disaster[1], forest management[2], traffic monitoring[4], and photogrammetry for 3D modeling[5]. Among them, 3D modeling combining SfM technology, which is a method of simultaneously restoring the three-dimensional shape of the shooting area and the position of the camera from multiple images shot while changing the camera's viewpoint, and low-level aerial shooting by UAV is drawing attention. Complex objects such as complex topography survey[6] and photogrammetry of ancient buildings[7] can be 3D modeled. Compared with manual surveying, it has low cost, high speed, high maneuverability, and high safety of the UAV system for collecting images.

In the construction industry, it is expected that construction sites will be aerial photographed by UAV and 3D modeled by SfM, so that it can be used for progress management of construction[8] and soil volume management at the time of earthwork[9]. However, construction machinery are constantly moving about in the construction sites during construction. Therefore, SfM cannot accurately generate 3D models of the construction sites. Because SfM performs 3D modeling by using feature points from each taken image. And SfM does not assume that there is anything moving within the shooting area. Hence, it is necessary to stop all works while UAV aerial shooting. And as it can take a few hours for UAV aerial shooting, it is difficult to shoot frequently at construction sites.

Thus, in this research, construction machinery are detected in advance from all images taken by UAV and removed from 3D modeling targets. After that, 3D modeling by SfM is performed, and improvement of accuracy of 3D modeling is aimed even under construction work situation.

2.2 Features used for construction machinery detection

In the computer vision community, many researches on object detection and human detection are done. In the construction field, the researchers focus on developing techniques for automated 2D detection of construction workers, equipment and machinery[10] [11]. Based on these results, improvement of productivity is expected by performing automatic tracking and evaluating construction performance.

As to the detection method, it can be divided into two methods, detection method using a background difference in time unit from movie[11] and detection method using features in each image or each frame of the movie[10]. In the method using the background subtraction, it is impossible to detect an object in the idling state, and it is impossible to detect from a still image.

For object detection methods using features in images, HOG features[10] [12], Haar-like features[13], EOH features[14] and Edgelets features[15] have been proposed as classifiers. Detectable objects are different for each features. The construction machinery under working changes its shape, such as changing the direction or moving the arm. HOG features have a longer calculation time compared with others and have low detection accuracy, but it can be detected even if there is some shape change in the detection object. Construction machinery detection method using HOG features have been proposed. Also, in order to improve the detection accuracy,

method for improving HOG features have also been proposed[3] [10].

In this study, Joint-HOG features[3] generated by patterning a plurality of HOG features with thresholds and performing Real AdaBoost in two stages were used for construction machinery detection.

3. Overview of the proposed method

In this research, our goal is as follows. Construction machinery are detected in advance from all images taken by UAV and removed from 3D modeling targets. After that, 3D modeling by SfM is performed, and improvement of accuracy of 3D modeling is aimed even under construction work situation.

The algorithm flow of the system developed in this study is shown in **Fig. 1**. Of this system, detection of construction machinery using the Joint-HOG features and generation of a mask images were performed by Visual Studio 2015. Creation of mask images were made using OpenCV 3.0 which is a computer vision library. And to create the 3D model, PhotoScan professional of Agisoft Corporation was used.
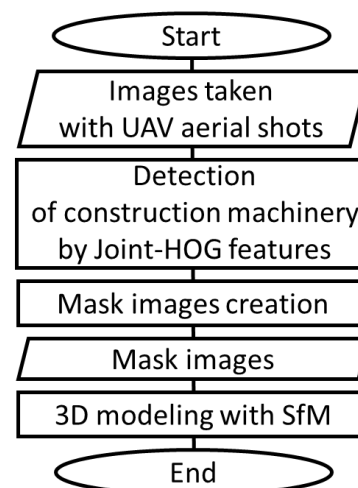
```
            Start
              |
      Images taken
   with UAV aerial shots
              |
         Detection
   of construction machinery
     by Joint-HOG features
              |
     Mask images creation
              |
         Mask images
              |
    3D modeling with SfM
              |
             End
```

Fig. 1. Algorithm flow of developed system.

3.1 Resource detection[3] [10]

The shape and appearance of construction

machinery can be characterized by distribution of local intensity gradients. These properties can be captured via HOG features[10) 12) 16)]. However, using single HOG features ends up to have low detection accuracy. In this study, Joint-HOG features[3)] generated by patterning a plurality of HOG features with thresholds and performing Real AdaBoost in two stages were used for construction machinery detection.

3.1.1 Histograms of Oriented Gradients (HOG) features

The flow of HOG features calculation is shown in **Fig.2**. The input image (**Fig. 2a**) is divided into cells containing arbitrary number of pixels, and gradient direction and brightness are calculated for each cell (**Fig. 2b**). Then, for each block composed of arbitrary cells, a histogram is generated (**Fig. 2c**), finally, normalization is performed for the entire detection window. The gradient strength of the luminance of the image L is m and the gradient direction is θ. Then, it is calculated from the following equations. Then, the obtained gradient direction θ is divided into nine groups every 20 degrees to create a histogram.

$$m(x,y) = \sqrt{f_x(x,y)^2 + f_y(x,y)^2} \qquad (1)$$

$$\theta(x,y) = \tan^{-1}\frac{f_y(x,y)}{f_x(x,y)} \qquad (2)$$

$$\begin{cases} f_x(x,y) = L(x+1,y) - L(x-1,y) \\ f_y(x,y) = L(x,y+1) - L(x,y-1) \end{cases} \qquad (3)$$

Then, for each block composed of arbitrary cells, a

histogram is generated (**Fig. 2b**). Finally, normalize the entire detection window with the following formula. Here, v is the HOG features, k is the number of HOG features in the block, and ϵ is a coefficient for preventing division by zero problems.

$$v = \frac{v}{\sqrt{\left(\sum_{i=1}^{k} v_i^2\right) + \epsilon}} \qquad (\epsilon = 1) \qquad (4)$$

3.1.2 Co-occurrence of HOG features

In order to capture the continuous edge of the construction machinery, in this research Joint-HOG features[3)] is used for detection. By simultaneously identifying based on co-occurrence expressions of multiple HOG features, it is possible to improve the identification accuracy of patterns that cannot be detected with single HOG features.

In order to calculate Joint-HOG features, single HOG features are selected from different cells ci and cj, and a binarization code s representing whether or not it is a construction machinery is calculated from the following equation. Co-occurrence of HOG features are an index number of the combination of features represented in binary notation. In this method, it is a combination of two types of HOG features, and takes four values.

$$s(V) = \begin{cases} 1 & p \cdot v_o > p \cdot \theta \\ 0 & \text{otherwise} \end{cases} \qquad (5)$$
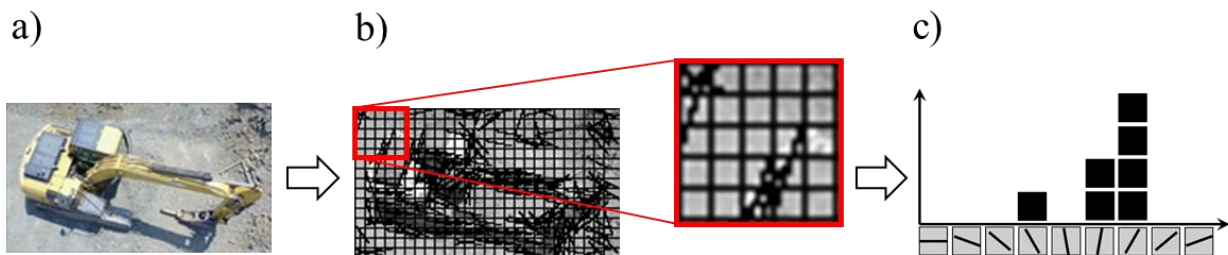

Fig. 2. Flow of HOG features extraction: (a) image example used for data set of construction machinery, (b) calculation of gradient direction and intensity of luminance, and (c) data of (b) shown in histogram.

3.1.3 Joint-HOG features

The co-occurrence expression of HOG features obtained in the previous section is used in the first stage Real Adaboost to generate the Joint-HOG features. First, an object suitable for Real AdaBoost is selected from the calculated Co-occurrence of HOG features. The weak classifier $h_t(x)$ of Real AdaBoost at the first stage is shown by the following equation. Here, $y_i \in \{+1, -1\}$ indicates the label of the correct answer, and the set of N labeled training samples is $(x_1, y_1), ..., (x_N, y_N)$. Also, t is the number of training rounds, and ϵ is a coefficient for preventing division by zero problems.

$$h_t(\mathrm{x}) = \frac{1}{2}\ln\frac{P_t(y = +1|j) + \epsilon}{P_t(y = -1|j) + \epsilon} \qquad (6)$$

$Pt(y = +1 \mid j)$ and $Pt(y = +1 \mid j)$ are conditional probabilities when observing the co-occurrence expression j of HOG features. The weights are initialized by $D_1(i)=1/N$. The above process is performed for all cell combinations.

$$P_t(y = +1|j) = \sum_{i:J_t(x_i)=j \wedge y_i=+1} D_t(i) \qquad (7)$$

$$P_t(y = -1|j) = \sum_{i:J_t(x_i)=j \wedge y_i=-1} D_t(i) \qquad (8)$$

$$D_{t+1}(i) = D_t(i)\exp[-y_i h_t(x_i)] \qquad (9)$$

Next, using the conditional probability distribution, we obtain the evaluation value z_1 representing the separation of the distribution by the following equation. Here, the distribution of the positive class and the negative class are far apart as the value of z_1 is smaller. The minimum value of z_1 is used to select weak classifiers in each round.

$$z_1 = 2\sum_j \sqrt{P_t(y = +1|j)P_t(y = -1|j)} \qquad (10)$$

Then, for all combinations of cells, a pool of Joint-HOG features, which is a strong classifier, is generated by Real AdaBoost of the first stage by the following equation. All of the generated Joint-HOG features generate the final classifier according to the following procedure.

$$H^{c_m,c_n}(x) = \sum_{t=1}^{T} h_t^{c_m,c_n}(x) \qquad (11)$$

First, the pool of Joint-HOG features are input, and probability density distributions $W+$ and $W-$ of positive and negative class are created. From the weight $Dt(i)$ of the learning sample i, it is obtained as a one-dimensional histogram by the following equation. The calculation formula of the weight $Dt(i)$ of the learning sample i is the same as that of the first stage Real AdaBoost. The number of BINs in the one-dimensional histogram is set to 64. And the created probability density distributions W_k^+, W_k^- are normalized so that the sum of the probability density distributions of each class becomes 1.

$$W_+^k = \sum_{i:k \in K \wedge y_i=+1} D_t(i) \qquad (12)$$

$$W_-^k = \sum_{i:k \in K \wedge y_i=-1} D_t(i) \qquad (13)$$

Based on the obtained probability density distribution, an evaluation value z_2 representing the degree of separation of the distribution is obtained. Here, the distribution of the positive class and the negative class are far apart as the value of z_2 is smaller. The minimum value of z_2 is used to select weak classifiers in each round.

$$z_2 = 2\sum_j \sqrt{W_+^k W_-^k} \qquad (14)$$

Then, $g_t(c)$ which is the weak classifier of Real AdaBoost of the second stage is calculated using the created probability density distribution W^k_+ and W^k_-. And the c is a number that represents combinations of cells. ϵ is a coefficient for preventing division by zero problems.

$$g_t(c) = \frac{1}{2}\ln\frac{W^k_+ + \epsilon}{W^k_- + \epsilon} \qquad (15)$$

Finally, with the Real AdaBoost of the second stage, only the effective features are selected from the pool of the Joint-HOG features calculated from the Real AdaBoost of the first stage to obtain the final strong classifier $G(c)$.

$$G(c) = \begin{cases} 1 & \sum_{t=1}^{T} g_t(c) > \lambda \\ 0 & \text{otherwise} \end{cases} \qquad (16)$$

3.2 Mask image creation

In the system developed in this research, construction machinery are removed from SfM 3D modeling area by creating mask images (**Fig. 3b**). Specifically, based on the Joint-HOG features obtained in the previous section, mask images are created for all images to be 3D modeled by SfM (**Fig. 3a**). Here, the mask images binarize the detected area of the construction machinery and the other areas. The

areas detected as construction machinery are excluded from 3D modeling by SfM. To create mask images, OpenCV 3.0 which is a computer vision library is used.

Even when the area other than the construction machine is erroneously detected as a construction machine or when the construction machine can not be detected, the created mask image is used as it is.

4. Experiment at construction site and validation metrics

To verify the proposed method, we conducted experiments on the construction site under working. In the demonstration experiment, there were two things done at the construction site. The first is construction machinery aerial shooting for creating data sets for benchmarking the visual detection of construction machinery. The second is the aerial shooting of a part of the construction site for 3D modeling by SfM. Then, after adapting the method proposed in this research to the construction site taken the second aerial shot, we made 3D modeling.

4.1 Generate identifier
4.1.1 Data collection and data set creation

All construction machinery working in the 3D modeling area by SfM were taken videos from multiple directions while changing brightness using a
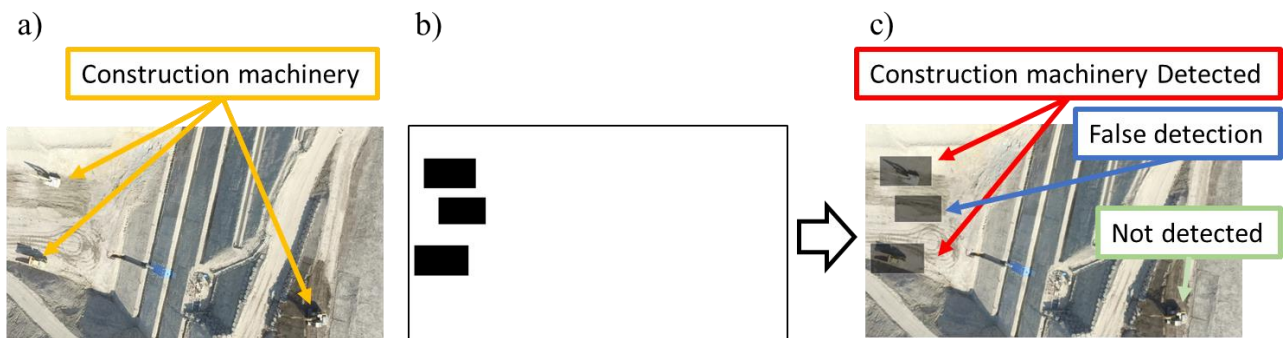

Fig. 3. An example of a mask image created by detecting a construction machinery based on Joint-HOG features: (a) Image used for 3D modeling by SfM, (b) Mask image, and (c) Image in which (a) and (b) are superimposed.

UAV, Mavic Pro of DJI. When construction machinery of the same company and of different sizes were counted as one type, there were fourteen construction machinery totaling eight types in total (**Fig. 4**). Breakdown of the eight types are backhoe (**Fig. 4a, 4b and 4c**), wheel roller (**Fig. 4d**), heavy dump (**Fig. 4e**), hydraulic breaker (**Fig. 4f**), bulldozer (**Fig. 4g**), dump truck (**Fig. 4h**). And digital images for creating data sets for benchmarking the visual detection of construction machinery were captured from the videos at 2.0fps. From the images, parts other than the construction machinery were trimmed as much as possible and resized to create eight kinds of positive data sets (80×45 pixels). For the negative data set (**Fig. 5**), 1,204 images obtained by trimming an area such as the ground and grass from the images obtained by imaging the 3D modeling area with UAV, Inspire1 of DJI, was used (80×45 pixels).

Fig. 4. Examples of positive datasets.

Fig. 5. Examples of negative datasets.

Table 1. The created data sets.

Types of data sets		Number of sheets
Positive	a	376
	b	230
	c	303
	d	216
	e	274
	f	291
	g	510

	h	208
Negative		1,204

4.1.2 Calculation of Joint-HOG features

Based on the created positive and negative data sets, joint-HOG features of eight types of construction machinery were calculated by the procedure described in the previous chapter. **Table 2** shows the parameters for Joint-HOG features calculation. Joint-HOG features calculated from positive data sets from a to h were taken as Joint-HOG from A to H, respectively. Then, the eight calculated Joint-HOG features were used as eight layers of construction machinery identifier (**Fig. 6**).

Table 2. Parameters for Joint-HOG features calculation.

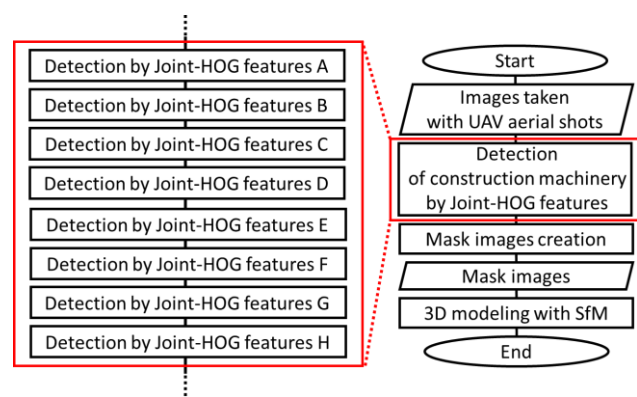|	Construction machinery
# of Orientations	9 (0° ～180°)
Patch size	80×45
Cell size	3
Block size	5
# cells	390
# of combinations	77,610

Fig. 6. Algorithm flow of construction machinery detection.

4.2 Objects to be 3D modeled

The object of 3D modeling is a part of the actual construction site. There were a total of fourteen construction machinery working in the 3D modeling

area (**Fig. 7**). The 3D modeling area was taken a video using UAV, Inspire1 of DJI. Aerial photographing by UAV was carried out during the day when construction work was carried out and the weather was sunny. The total flight distance of UAV was 646 m and the flight time was five minutes (**Fig. 8**). And 715 digital images (3840 × 2160 pixels) used 3D modeling by SfM were captured from the video at 2.0fps. Here, the 715 images are referred to as "original images".
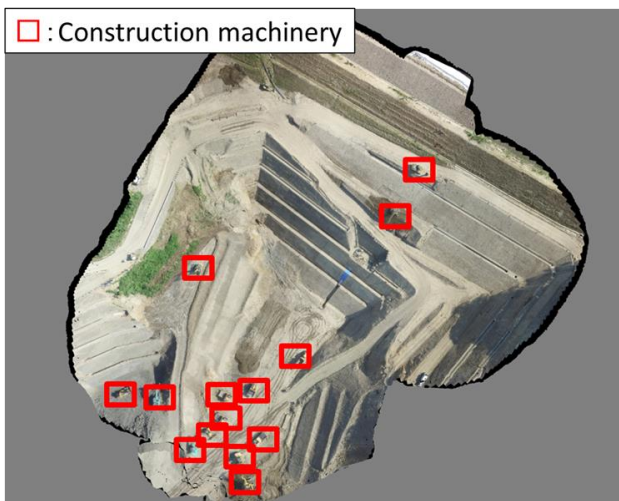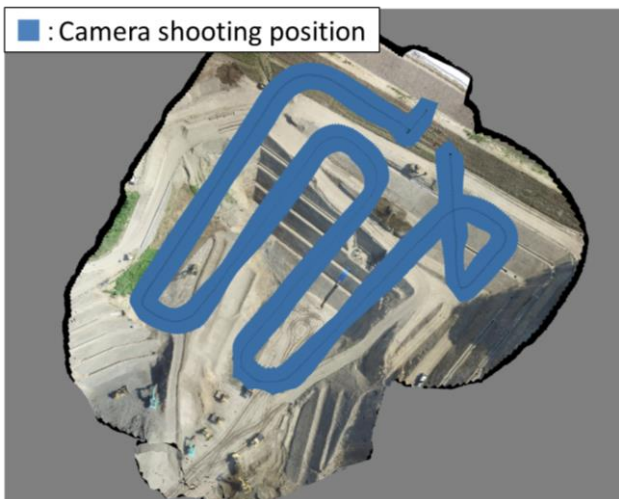

Fig. 7. Work position of construction machinery.

Fig. 8. 3D modeling area and UAV flight path.

4.3 Mask image creation

By using Joint-HOG features calculated in Chapter 4, Section 1, Subsection 2, construction machinery

were detected from the 715 original images, and a mask image was created for each image.

4.4 Detection of construction machinery by Joint-HOG features and 3D modeling by SfM

Finally, 3D modeling by SfM using PhotoScan pro was done twice, the first is for original images and the second is for images applied the developed system to original images. Here, "original images" indicate 715 images of a part of the construction site created in the previous section. Then, we output 3D model and point cloud data respectively from the created model.

5. Experimental result
5.1 Detection of construction machinery by Joint-HOG features

The detection rate of fourteen construction machinery was on average 54.5%. Also, the proportion of images including erroneous detection was 5.1%, and the proportion of images including undetected was 32.3%.

5.2 3D model and point cloud data

Fig. 9 shows a 3D model created from original images. **Fig. 10** shows a 3D model created from images applied the developed system to original images. And **Fig. 11** shows expand part of **Fig. 9** (**A**) and **Fig.10** (**B**). And (**A´**) and (**B´**) are single color solid models. In **Fig. 11**, two construction machinery are included, respectively. From these, it can be confirmed that the 3D model created from images applied the developed system to original images has a smaller part of the construction machinery than the 3D model created from original images.

Fig. 12 is a diagram in which two output 3D point cloud data are superimposed. Then, the difference between the distances between the nearest points of the two three-dimensional point cloud data is indicated by a histogram. As shown in **Fig. 12**, the dif-

Fig. 9. 3D model created from original images.

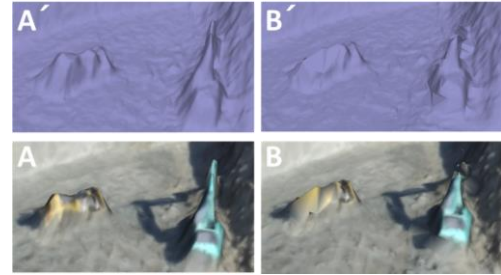**Fig. 10**. 3D model created from images applied the developed system to original images.

Fig. 11. Expand part of Fig. 9 and 10: (A´) and (B´) are single color solid models.

ference in the distance between the nearest neighbor points was large at the part where the construction machinery was present, and it was confirmed that the accuracy of 3D modeling was improved by the developed system.
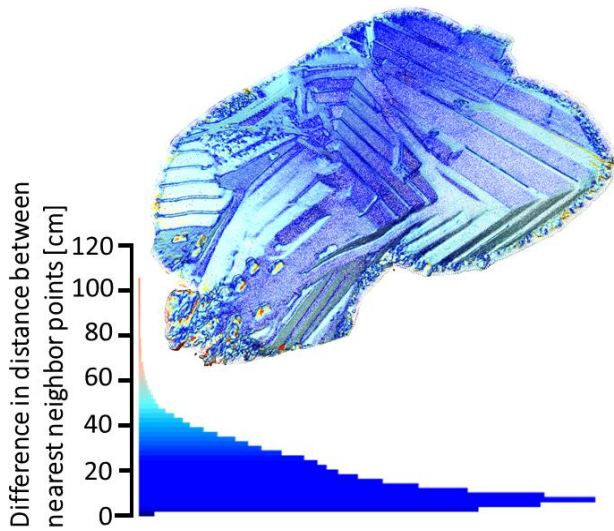

Fig. 12. Difference of nearest neighbor points between created models.

6. Conclusion

In this paper, 3D modeling at construction sites by SfM, we developed a system for 3D modeling after detecting construction machinery based on Joint-HOG features and creating mask images to remove construction machinery from images used for 3D modeling. The conclusion of this study is as follows.

· Joint-HOG features can be used as a classifier of construction machinery. The detection rat was on average 54.5%. Also, the proportion of images including erroneous detection was 5.1%, and the proportion of images including undetected was 32.3%.

· With the developed system, we confirmed the improvement of the 3D modeling accuracy in the situation where the construction machinery working in the shooting area.

In addition, by increasing the detection rate, it is expected that noise of construction machinery can be removed more in 3D modeling. In the future, we will aim for not only construction machinery but also workers and other 3D modeling error factors to extend the removal target and improve the detection rate.

Acknowledgment

References

1) F. Yamazaki, T. Matsuda, S. Denda, and W. Liu, Construction of 3D models of buildings damaged by earthquakes using UAV aerial images, *Proceedings of the Ninth Pacific Conference on*

Earthquake Engineering, Paper No. 204, 2014.

2) T. Tamura, A. Kato, H. Obanawa and T. Yoshida, 2015. Three height measurement from areal images taken by a small Unmanned Aerial Vehicle using Structure Motion, *J. Jpn. Soc. Reveget. Tech*, 41(1):163-168.

3) T. Mitsui, Y. Yamauchi and H. Fujiyoshi, 2009. Object Detection by Two-Stage Boosting with Joint Features, *The IEICE Transactions on Information and Systems*, 92(9):1591-1601.

4) F. Heintz, P. Rudol, P. Doherty, From images to traffic behavior—a UAV tracking and monitoring application, *10th International Conference on Information Fusion, IEEE*, 2007.

5) F. Remondino, L. Barazzetti, F. Nex, M. Scaioni, and D. Sarazzi, 2011. UAV photogrammetry for mapping and 3d modeling–current status and future perspectives, *International Archives of the Photogrammetry, Remote Sensing and Spatial Information Sciences*, 38(1), C22.

6) S. Lee and Y. Choi, 2015. Topographic survey at small-scale open-pit mines using a popular rotary-wing unmanned aerial vehicle (drone), *Tunnel and Underground Space*, 25(5): 462-46.

7) SG. Barsantia, F. Remondino, and D. Visintini, 2013. 3D Surveying and Modelling of Archaeological Sites-some critical issues, *ISPRS Photogrammetry, Remote Sensing and Spatial Information Sciences*, 2-6.

8) M. Golparvar-Fard, F. Peña-Mora, CA. Arboleda, and S. Lee, 2009. Visualization of construction progress monitoring with 4D simulation model overlaid on time-lapsed photographs, *Journal of Computing in Civil Engineering*, 23(6):391-404.

9) YS. Cho, NY. Lim, WS. Joung, SH. Jung and SK. Choi, 2014. Management of Construction Fields Information Using Low Altitude Close-range Aerial Images, *Journal of the Korean Society of Surveying, Geodesy, Photogrammetry and Cartography*, 32(5):551-560.

10) M. Memarzadeh, M. Golparvar-Fard and JC. Niebles, 2013. Automated 2D detection of construction equipment and workers from site video streams using histograms of oriented gradients and colors, *Automation in Construction*, 32:24-37.

11) S. Chi and CH. Caldas, 2011. Automated object identification using optical video cameras on construction sites. *Computer‐Aided Civil and Infrastructure Engineering*, 26(5):368-380.

12) Q. Zhu, MC. Yeh, KT. Cheng, and S. Avidan, Fast human detection using a cascade of histograms of oriented gradients. *In Computer Vision and Pattern Recognition*, *IEEE Computer Society Conference on*, Vol. 2, pp. 1491-1498. 2006.

13) P. Viola, MJ. Jones and D. Snow, Detecting pedestrians using patterns of motion and appearance, *IEEE International Conference on Computer Vision*, pp.734-741, 2003.

14) K. Levi and Y. Weiss, Learning object detection from a small number of examples: the importance of good features, *Proceedings of the 2004 IEEE Computer Society Conference*, pp. 53-56, 2004.

15) B. Wu, R. Nevatia, Detection of multiple, partially occluded humans in a single image by bayesian combination of edgelet part detectors. *International Conference on Computer Vision, Beijing*, pp. 90-97, 2005.

16) N. Dalal and B. Triggs, Histograms of oriented gradients for human detection, *Proc. IEEE Conf. Computer Vision and Pattern Recognition*, pp. 886-893, 2005.